0026-895X/92/050845-11$03.00/0

MOLECULAR PHARMACOLOGY, 41:845-855

DNA-Binding Properties of a Distamycin-Ellipticine Hybrid Molecule

CHRISTIAN BAILLY, COLM O'HUIGIN, RAYMOND HOUSSIN, PIERRE COLSON, CLAUDE HOUSSIER, CHRISTIAN RIVALLE, EMILE BISAGNI, JEAN-PIERRE HENICHART, and MICHAEL J. WARING

University of Cambridge, Department of Pharmacology, Cambridge CB2 1QJ, UK (C.B., C.O., M.J.W.), INSERM U16, 59045 Lille, France (C.B., R.H., J.-P.H.), Laboratoire de Chimie Macromoléculaire et Chimie Physique, Université de Liège, 4000 Liège, Belgium (P.C., C.H.), and UA533 CNRS, Laboratoire de Synthèse Organique, Institut Curie, Section Biologie, 91405 Orsay, France (C.R., E.B.)

Received October 17, 1991; Accepted January 20, 1992

SUMMARY

We have synthesized a distamycin-ellipticine hybrid compound and investigated its interaction with DNA, using various optical and gel electrophoresis techniques. Binding of the hybrid to DNA is evidenced by spectral shifts, fluorescence quenching, and induced linear dichroism. Absorbance measurements have been used to generate Scatchard plots, which reveal that the interaction cannot be described adequately in terms of a single binding mode, probably because of simultaneous intercalation and minor groove binding of the ligand. Competition with added distamycin has been used to verify involvement of the *N*-methyl-pyrrole portion of the hybrid molecule in the binding reaction. From electric linear dichroism experiments, it is estimated that the orientation of the DNA-bound ellipticine chromophore in the hybrid differs by about 10° from the orientation of the equivalent chromophore lacking a distamycin tail. Topoisomerase assays establish that binding of the hybrid unwinds the DNA helix by a minimum of 11°, which is consistent with intercalation but notably smaller than the unwinding angle of ellipticine. In footprinting experiments, it is found that the AT- and GC-specificity of distamycin and ellipticine, respectively, appear to be merged in the binding of the hybrid, which produces a pattern of protection distinct from the characteristic patterns for either of the parent compounds. The hybrid is an extremely effective inhibitor of cutting by DNase I.

Modifications of the sequence and/or structure of DNA have been implicated in the initial stages of complex biological processes leading to many cellular dysfunctions such as cancer. The discovery of oncogenes, and how they may be activated in cancer cells, certainly stands as one of the best examples (1). At the same time, normal cellular functioning involves the action of specific DNA-binding regulatory proteins. These proteins bind with marked sequence specificity to the transcriptional control regions of particular genes (2). The problem at hand is, firstly, to determine whether the particular DNA sites involved in a defined pathology are accessible to manipulation and, secondly, to design drugs that can target such sites.

Strategies for targeting based on synthetic nonprotein ligands, which through their base-specific interaction with DNA would mediate a desirable biological response or abolish an undesirable biological process, have been evolving during the last few years (3, 4). It is essentially the discovery of natural toxins that has initiated the research on nonprotein DNA-effector molecules. More and more active molecules have been identified, which may be classified into three groups, intercalators, alkylators, and minor groove binders. Within each group, extensive structure-activity relationships have been elucidated. They allow us to discern chemical rules applicable to molecular recognition of DNA, which are essential for a future rational design. Recently, using these rules, an approach based on ligands of mixed binding capacities has been tried. Intercalators linked to an alkylating drug (5–7), minor groove binders linked to an alkylator (8–10), and minor groove binders attached to an intercalating nucleus (3, 11–14) have been reported. Intercalators, alkylators, and minor groove binders perturb DNA structure in very different ways (15). The coupling of two different DNA-binding units thus presents a challenge with important potential consequences.

In the present work, we have studied a new synthetic hybrid drug bearing a distamycin moiety covalently tethered to an ellipticine moiety (Fig. 1). Distamycin, along with its congener netropsin, is the archetype of the groove binder. Distamycin binds to DNA within the minor groove by replacing its spine of hydration and strongly favors AT-rich regions of DNA as its binding sites (particularly the 5′-AATT-3′ site) (16). Ellipti-

This work was supported by grants to M.J.W. from the Cancer Research Campaign, the Medical Research Council, and the Royal Society; to J.-P.H. from the Institut National de la Santé et de la Recherche Médicale and the Association pour la Recherche sur le Cancer; to E.B. from the Centre National de la Recherche Scientifique and the Institut Curie; to C.H. from the Services de Programmation de la Politique Scientifique (ARC Contract 80/85–90); and from the Fonds National de la Recherche Scientifique (FRFC Convention 2.4501.91).

ABBREVIATIONS: ELD, electric linear dichroism; CT, calf thymus; D/P ratio, drug/DNA phosphate ratio.

cines are well known intercalators (17), which often also induce protein-associated DNA strand breaks (18); they can also bind covalently to DNA after a biooxidative process (19).

The distamycin moiety has been linked to a 9-methoxy ellipticine derivative by a short spacer aminopropylamino grouping at position 1. 9-Methoxy 1-aminoalkylamino ellipticines are, to date, the most active ellipticine derivatives known, so our hybrid compound could be of biological interest as an anticancer or an antiviral drug. The choice of this particular ellipticine derivative was made also on the basis of our recent findings that this compound binds to DNA with a marked GC preference (20). In view of the different sequence specificities of its constituent moieties, it is compelling to know which, if any, of the specificities are found for the hybrid.

In the present study, we have investigated the strength and mode of binding of this hybrid molecule to DNA by using various spectroscopic techniques (including absorption, fluorescence, and ELD) and by using a topological method to assay the relative ability of the drug to unwind supercoiled DNA. The sequence specificity of binding was determined by DNase I footprinting experiments.

Materials and Methods

Chemicals. Distamycin A hydrochloride was purchased from Boehringer Mannheim; stock solutions were prepared in water. The 1-substituted ellipticine derivative was obtained by reaction of 1-chloro-5,11-dimethyl-9-methoxy-ellipticine with diaminopropane, as previously described (21); stock solutions were prepared in methanol and stored at −20° in the dark.

The synthesis of the hybrid drug, together with complete spectral characterization, will be reported in a chemical communication. Briefly, the drug was obtained from the coupling of 4-[[4-[[4-[(formylamino)-1-methyl-pyrrol-2-yl]carbonyl]amino]-1-methyl-pyrrol-2-yl]carbonyl] amino-1-methyl-pyrrol-2-carboxylic acid (12) with 1-(amino-3-propylamino)-5,11-dimethyl-9-methoxy-6*H*-pyrido[4,3-*b*]carbazole (21). Stock solutions of this compound were prepared in dimethylformamide before subsequent dilutions with water. The final methanol or dimethylformamide concentrations did not exceed 1–2% (v/v) and were found not to affect cleavage of a restriction fragment by DNase I.

Biochemicals. CT DNA (highly polymerized sodium salt) and poly[d(AT)·d(AT)] were purchased from Sigma Chemical Co. and used without further purification. Their concentrations, expressed with respect to nucleotides, were determined using extinction coefficients (ϵ) at 260 nm equal to 6600 and 6700 M^{-1} cm^{-1}, respectively.

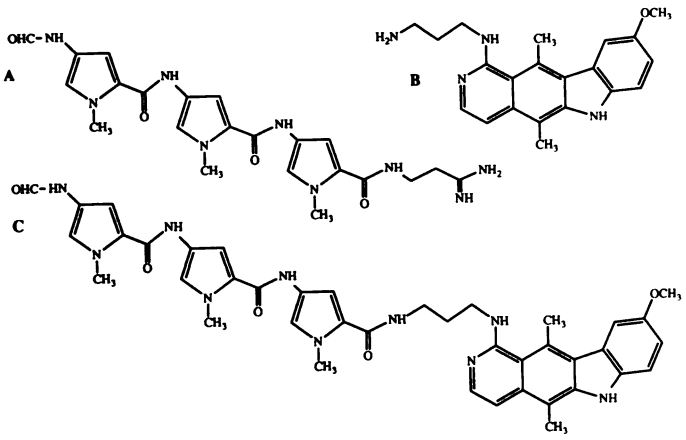

Fig. 1. Chemical structures of distamycin A (A), the ellipticine derivative (B), and the distamycin-ellipticine hybrid drug (C).

For DNA relaxation experiments, the plasmid pKMΔ-98 was used. It was isolated from *Escherichia coli* by an alkaline lysis procedure and was purified by banding twice in CsCl-ethidium bromide gradients, as previously described (22, 23). Ethidium was removed by several isopropanol extractions, followed by exhaustive dialysis against TE buffer to remove the CsCl.

For the footprinting studies, the 160-base pair *tyr* T DNA fragment containing the tyrosine tRNA promoter was isolated from the plasmid pKMΔ-98 and labeled according to previously published procedures (22, 23). Incubation with the Klenow fragment of DNA polymerase (Boehringer) and [α-^{32}P]dCTP led to selective labeling of the 3′-end of the top strand (Watson strand), whereas incubation with [α-^{32}P]dATP led to selective labeling of the 3′-end of the bottom strand (Crick strand). Restriction enzymes and topoisomerase I were purchased from New England Biolabs and BRL, respectively, and were used according to the manufacturer's instructions. The radioactive nucleotides (6000 Ci/mmol) were from New England Nuclear.

Buffers. The buffers used for spectroscopic DNA binding analysis contained 1 mM Tris·HCl, pH 7.0, or 25 mM potassium phosphate adjusted to pH 7.0 by mixing KH_2PO_4 and K_2HPO_4. Solutions of DNA were prepared in the desired buffer for each titration. The drugs were found to obey Beer's law at concentrations used for DNA binding analysis (generally up to 5 μM). Footprinting experiments were performed in 10 mM Tris·HCl buffer, pH 7.0, containing 10 mM NaCl. Electrophoresis was carried out in TBE buffer (8.9 mM Tris base, 8.9 mM boric acid, 2.5 mM Na_2EDTA, pH 8.3).

Absorption spectroscopy. Absorption spectra were recorded on a Uvikon-Kontron 810–820 spectrophotometer coupled to a Uvikon recorder 21 and a Uvikon thermoprinter 48. The cell holder (10-mm path length) was thermostated with a Haake unit. Titrations of the drugs with DNA, covering a large range of D/P ratios, were performed by adding aliquots of a concentrated DNA solution to another solution at constant drug concentration. Such procedures avoid adhesion of the drugs to the cuvettes. For melting temperature studies, heating rates of 1°/min were used, and drug-DNA complexes were prepared by adding drug stock solutions to 50 μM CT DNA or 20 μM poly[d(AT)·d(AT)] solutions in 0.1 × standard saline citrate (1.5 mM sodium citrate, 15 mM sodium chloride) buffer, to obtain D/P ratios varying from 0 to 1. Measurements were carried out at 260 nm.

Fluorescence studies. All fluorescence spectra were recorded on a Kontron SFM25 spectrofluorimeter and are uncorrected. To a dilute drug solution (5 μM), a concentrated DNA solution was added in small aliquots. The blank signal obtained with DNA alone was <0.5% of that with the drugs. For competition experiments, small aliquots of distamycin (3 μl) from a concentrated solution were added to 3 ml of hybrid-DNA and ellipticine-DNA solutions. Spectra were recorded after 10 min of equilibration.

ELD. ELD was measured as previously described (13).

Binding constants and estimates of site size. Binding constants and site-size estimates were determined using experimental spectrophotometric readings from absorbance titration experiments conducted at 325 nm with distamycin, 322 nm with the ellipticine derivative, and 323.5 nm with the hybrid molecule. For each ligand, the apparent association constant(s), K (M^{-1}), and parameter(s) of site size, $1/n$ (in nucleotides), were estimated from Scatchard plots using both of two models, firstly, the noncooperative ligand binding model of McGhee and von Hippel (24) and, secondly, a two-site model that assumes the existence of two independent noncooperative types of binding sites (13). The program Enzfitter (Elsevier Biosoft) (25) was used to secure the best fit of the data to these two models.

DNA unwinding experiments. Unwinding experiments were carried out according to a published procedure (26). Supercoiled pKMΔ-98 (0.6–0.8 μg) was incubated with CT DNA topoisomerase I (3 units) at 37° for 4 hr, in relaxation buffer (50 mM Tris, pH 7.8, 50 mM KCl, 10 mM $MgCl_2$, 1 mM dithiothreitol, 1 mM EDTA), in the presence of varying concentrations of the drug under study. Reactions were terminated by extraction with neutralized phenol. DNA samples were

then added to the electrophoresis dye mixture (3 μl) and electrophoresed (35 V/cm) in a 0.9% agarose gel at room temperature for 15 hr. Gels were stained with ethidium bromide (1 μg/ml), washed, and photographed under UV light.

DNase I footprinting, gel electrophoresis, and data processing. The procedure for footprinting experiments was exactly as previously described (22, 23). The cleavage products of the nuclease reactions were analyzed on 0.3-mm-thick 8% polyacrylamide gels containing 8 M urea and TBE buffer. After 2 hr of electrophoresis at 1500 V, the gels were soaked in 10% acetic acid for 15 min, transferred to Whatman 3MM paper, dried under vacuum at 80°, and subjected to autoradiography at −70°, with an intensifying screen. Autoradiographs were scanned using a multichannel computer-operated gel scanner at the Medical Research Council Laboratory of Molecular Biology (Cambridge, UK), by kind permission of Sir Aaron Klug and Dr. J. M. Smith. Gel profiles were plotted and displayed on a raster graphics screen. Quantitative analysis of the gel electrophoresis profiles was performed by integration of the area under each peak, using a computer program developed specially for the purpose (27). The area under each peak was integrated by simple addition of the pixels under the curve. Data are presented in the form $\ln(f_a) - \ln(f_c)$, representing the differential cleavage at each bond relative to that in the control (f_a is the fractional cleavage at any bond in the presence of the drug and f_c is the fractional cleavage of the same bond in the control). The results are displayed on a logarithmic scale for the sake of convenience.

Results

Absorption studies. Fig. 2 displays the spectral changes that occur at low ionic strength when distamycin, ellipticine, and the hybrid drug are added to CT DNA. A bathochromic shift and hypochromism are observed. The interaction of distamycin with CT DNA causes a displacement of 18 nm in the absorption maximum, owing to the perturbation of the complexed chromophore system after binding to DNA. A nearly

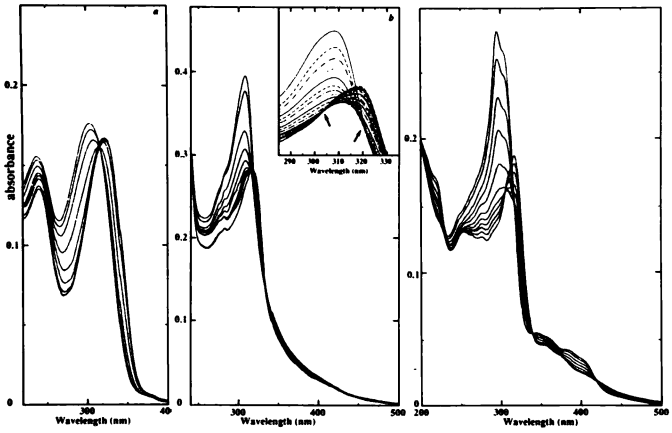

Fig. 2. DNA titrations of distamycin (a), the hybrid (b), and the ellipticine derivative (c), under low ionic strength conditions. The figure contains the absorption spectra of the free drug (5 μM), intermediate spectra, and final spectra of the drug-DNA complexes, in which the ligands have been sequestered completely by the DNA. A titration consisted of 15–20 spectral measurements; however, some intermediate spectra have been omitted from this figure for clarity. To 3 ml of drug solution (5 μM in 1 mM Tris·HCl buffer, pH 7.0) were added successive amounts of CT DNA. Spectra are referenced against DNA solutions of exactly the same DNA concentration and were adjusted to a common base line at 550 nm. The phosphate-DNA/drug ratio increased as follows (*top* to *bottom curves*, at 280 nm): a, 0, 0.5, 1, 2, 2.5, 3.5, 5, and 10; b, 0, 0.3, 0.6, 0.9, 1.2, 1.5, 2, 2.5, 3, and 5; c, 0, 0.4, 0.8, 1.2, 1.6, 2, 2.4, 2.8, 3.2, 3.6, and 4. b, *inset*, spectral shifts of the hybrid upon titration with CT DNA, using the same scale of absorbance but an expanded wavelength scale. *Arrows*, the two isosbestic points.

isosbestic point is observed at 313 nm and is maintained even at higher ionic strengths.

With the ellipticine moiety alone, at high D/P ratios four isosbestic points, at 227, 317, 336, and 416 nm, are seen, and a hypochromic effect is observed at 300 nm, without any significant red shift. Subsequent additions of DNA induce dramatic changes of the UV spectra. The isosbestic point at 317 nm disappears and an increase of absorbance at this wavelength is observed. A red shift of 12 nm occurs rapidly, together with a small hyperchromic effect centered around 317 nm. A new isosbestic point is observed at 304 nm. This second state, occurring at higher DNA/drug ratio, could reflect the transition of the externally binding drug to an intercalated form. Thus, at this low ionic strength, the optical changes associated with the binding of the ellipticine moiety to DNA clearly point to the existence of two distinct binding modes. Most likely, an externally bound cation moves into the interior of the double helix as the availability of free binding sites increases.

The titration of this 1-aminopropylamino-substituted ellipticine with CT DNA is apparently different from that reported by Paoletti and colleagues (28) for the unsubstituted ellipticine base. There, a simpler evolution of the spectra was reported, whereas here the spectral behavior is much more complex. When the titrations with our ellipticine derivative are repeated at higher ionic strength (25 mM potassium phosphate buffer, pH 7.0), a single, constant, isosbestic point is observed, similar to that seen with the natural ellipticine chromophore (data not shown). It appears that an outside binding process observed at low ionic strength is favored by the presence of the 1-aminopropylamino side chain, which can also interact with DNA phosphate, via electrostatic bonds, or perhaps with base pairs protruding into the groove of the double helix.

Titration of the distamycin-ellipticine hybrid with CT DNA under identical conditions shows similar biphasic evolution of the UV spectra (see Fig. 2b, *inset*). An isosbestic point is first observed at 318 nm, at a P/D ratio of <1. Subsequent UV curves intersect each other at a lower wavelength, indicating the presence of a second isosbestic point at 307 nm. By comparison with the behavior of the ellipticine derivative alone, this suggests that at low ionic strength an external binding occurs first, before intercalation of the ellipticine chromophore of the hybrid. Indeed, the putative two-step binding process is surely due to the fixation of the ellipticine moiety of the hybrid, because a one-step binding process is observed with distamycin whatever the ionic strength. It is already obvious at this stage that the binding of the distamycin moiety does not disturb the DNA-binding of the ellipticine moiety.

The titration of the hybrid drug with CT DNA at higher ionic strength (25 mM potassium phosphate buffer, pH 7.0) reveals the presence of a single isosbestic point at 318 nm, which attests to the loss of the first binding step, i.e., the external binding (data not shown). With respect to changes in the UV spectrum of the hybrid, the absorption band centered at 306 nm corresponds to an overlap of the distamycin and ellipticine chromophores of the molecule in such a way that the observed modifications cannot be clearly attributed to one or another part of the ligand. However, the observation of a single isosbestic point at medium ionic strength is consistent with the involvement of only one DNA-binding process. Extinction coefficients and related spectral data are summarized in Table 1.

Binding affinity. The affinity constant of hybrid com-

TABLE 1
Spectral characteristics of ligand-DNA complexes

Ligand	Absorption[a]				Fluorescence[b]				Unwinding angle[c]
	Free		Bound		Free		Bound		
	λ_{max}	ϵ	λ_{max}	ϵ	λ_{max}	RFI	λ_{max}	RFI	
	nm	$M^{-1}\,cm^{-1}$	nm	$M^{-1}\,cm^{-1}$	nm		nm		
Distamycin	302	35,000	320	29,400					
Ellipticine derivative	306	48,000	318	25,900	445	103	492 523	109 105	19°
Hybrid	306	81,000	322	59,360	445	56	488 517	135 120	11°

[a] λ_{max}, absorption maximum; ϵ, molar extinction coefficient.
[b] RFI, relative fluorescence emission intensity measured with excitation at 318 nm.
[c] Helical unwinding per added drug molecule, determined from different gels, as illustrated in Fig. 7.

pounds for DNA cannot be simply deduced from binding measurements using Scatchard analysis applied to a single binding site. Studies with a netropsin-acridine hybrid (13) have shown that two types of binding can coexist, one corresponding to minor groove binding and intercalation simultaneously and the other to minor groove binding only. By assuming two independent noncooperative types of interaction, the binding curves can be fitted by the equation $r/c = [(n_1K_1)/(1 + c\ K_1)] + [(n_2K_2)/(1 + c\ K_2)]$, where r represents the total observed binding stoichiometry, c is the concentration of the free ligand, n_1 and n_2 represent the numbers of ligand binding sites per nucleotide for modes 1 and 2, respectively, and K_1 and K_2 are the corresponding association constants.

We have applied this analysis to the spectrophotometric data for the present distamycin-ellipticine hybrid, despite some misgivings that the manifest complexity of the spectral behavior might vitiate the derived binding parameters. At the same time, we attempted to secure an acceptable fit to the data using McGhee-von Hippel analysis (24).

Scatchard plots for all three compounds can be satisfactorily fitted by curves corresponding to the two-site model, but with distamycin there is no advantage of two-site analysis over the more orthodox McGhee-von Hippel method and, indeed, the latter yields a better curve on visual inspection (Fig. 3). In contrast, the data for the ellipticine derivative, as well as for the hybrid, deviate seriously from any theoretical curve plotted according to the McGhee-von Hippel equation (24) and are obviously much better fitted by the two-site model.

Binding parameters resulting from these efforts are collated in Table 2. They reveal that, as judged by any criterion, the strength of binding of the hybrid to DNA is not much different from that of the ellipticine derivative alone, nor are there any great differences in the calculated values for binding site size. Binding constants are often thought to be multiplicative, but there is no evidence of such an effect here; assuming that both intercalation and minor groove binding are occurring together, they do not result in enhanced binding of the hybrid. It is interesting that McGhee-von Hippel analysis indicates an increase in the binding site size ($1/n$) for the hybrid, as one might intuitively expect, but the two-site model is ambiguous with respect to any effect of this sort. Otherwise, the binding constants and site sizes calculated for the ellipticine derivative and for distamycin fall within the range of reported values (17, 28, 29).

Fluorescence studies. To elucidate the DNA binding process further, fluorescence titrations were performed, taking advantage of the high fluorescence quantum yield of the ellipticine chromophore. This effectively provides a means of monitoring the behavior of the ellipticine moiety of the hybrid, with no significant contribution from the distamycin moiety to the measured signal.

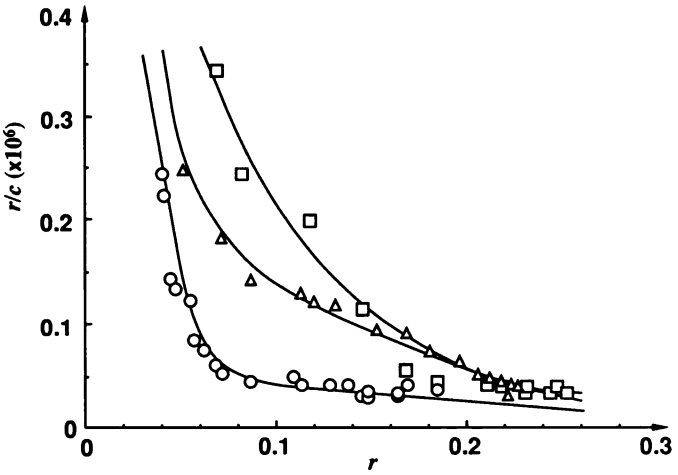

Fig. 3. Representative Scatchard plots for the evaluation of the binding of distamycin (□), the ellipticine derivative (△), and the hybrid (○) to CT DNA. The *symbols* represent the uncorrected experimental points, and the *curves* for the ellipticine derivative and the hybrid represent the best fit to the equation for two independent noncooperative binding sites, with the binding parameters given in Table 2. The curve for distamycin is a McGhee-von Hippel curve (24) characterized by the values recorded in Table 2.

Fig. 4 shows the emission and excitation spectra of the hybrid and of the ellipticine derivative, in the absence and presence of DNA, at medium ionic strength (25 mM phosphate, pH 7.0). With the ellipticine derivative, addition of DNA results in a decrease of the fluorescence excitation intensity at 288 nm and increased intensity at 315 nm; similarly, with the hybrid the excitation intensity increases at 315 nm (the emission wavelength was set at 500 nm).

When DNA is added to a solution of the ellipticine derivative, the shape of the emission spectrum changes from a single broad peak centered around 445 nm to a doublet with maxima at 492 nm and 523 nm, of almost equal fluorescence intensity. The spectra do not intersect each other so as to form a well defined isosbestic point but delineate a crossover region near 470 nm. This is in general agreement with the predominance of one binding mode (intercalation), as postulated from the absorption studies at this ionic strength.

The interaction of the hybrid compound with DNA results

TABLE 2

Association constant, *K*, and number of ligand binding sites per nucleotide, *n*

Ligand	Two-site model					McGhee-von Hippel model		
	K_1	n_1	K_2	n_2	χ^2	K	n	χ^2
	M^{-1}		M^{-1}			M^{-1}		
Distamycin						$5.7 \pm 0.5 \times 10^5$	0.274 ± 0.015	5.8×10^{-4}
Ellipticine derivative	$1.5 \pm 0.2 \times 10^8$	0.048 ± 0.006	$3.0 \pm 0.4 \times 10^5$	0.32 ± 0.006	4.2×10^{-5}	$3.8 \pm 0.6 \times 10^5$	0.385 ± 0.04	6×10^{-3}
Hybrid	$9 \pm 4 \times 10^7$	0.035 ± 0.010	$9.4 \pm 6.0 \times 10^4$	0.38 ± 0.15	8.4×10^{-5}	$2.1 \pm 0.3 \times 10^5$	0.222 ± 0.025	1.2×10^{-3}

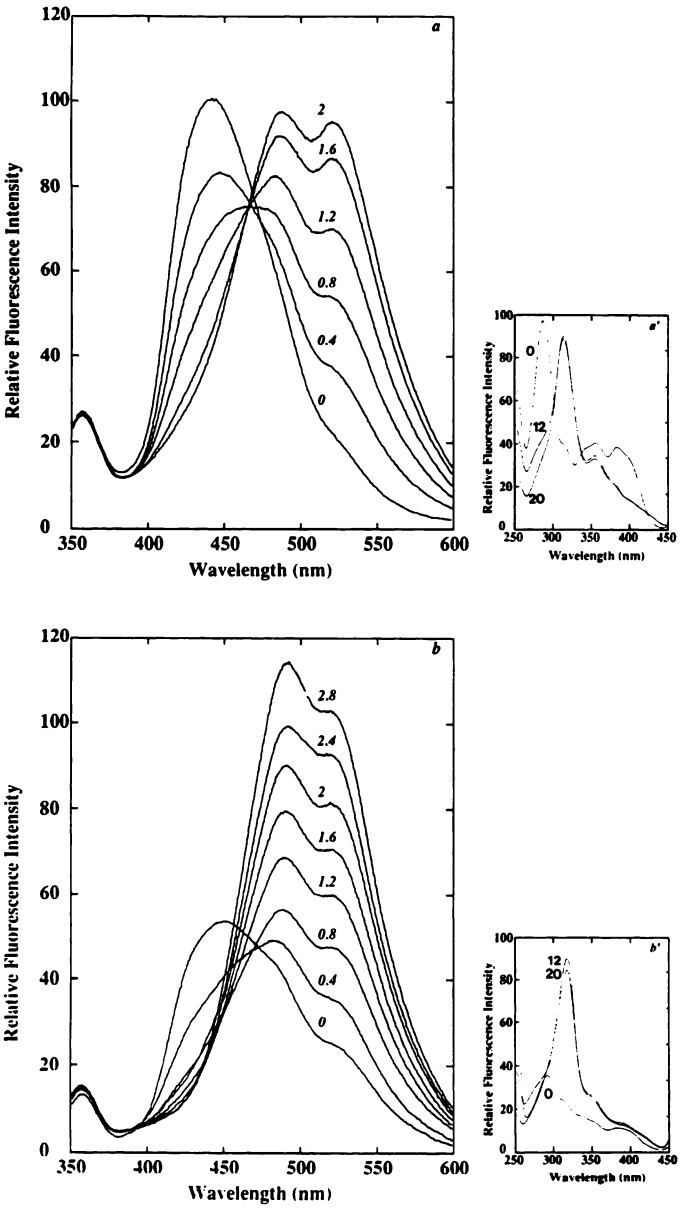

Fig. 4. Fluorescence emission (a and b) and fluorescence excitation (a′ and b′) spectra of the ellipticine derivative (a) and the hybrid (b), in the absence and presence of CT DNA, at pH 7.0, in 25 mM phosphate buffer. The fluorescence emission spectra were recorded with an excitation wavelength of 318 nm, which corresponds to the isosbestic point observed in the absorption spectrum (see Fig. 2). The excitation spectra were obtained with the emission monochromator set at 500 nm for both bound and free drug. A flat line at practically zero fluorescence intensity was observed without drugs and in the presence of DNA. Spectra in a and b have been recorded on the same scale and can be compared directly. DNA phosphate/drug ratio is indicated for each spectrum.

in a red shift of the fluorescence maximum from 445 nm to 488 nm. The emission spectrum of the DNA-bound hybrid ligand corresponds to a doublet in which the peak at 488 nm predominates over that at 518 nm. Upon titration with DNA, at high D/P ratio, the curves intersect at a position close to that observed with the ellipticine moiety alone (near 488 nm), which indicates similar intercalative binding. At lower D/P ratio, the intersection of the curves delineates a crossover region around 440 nm. The divergence of this point from the first one probably indicates the appearance of a different mode of binding, involving the distamycin part of the molecule.

The ratio of the fluorescence intensity of bound to free drug was found to be different for the ellipticine moiety and the hybrid (Table 1). At pH 7.0, the fluorescence intensity of the fully DNA-bound hybrid increased 2.4-fold, compared with that of the free molecule in solution, whereas for the ellipticine derivative the intensity hardly changed at all.

Competition experiments. In order to probe the influence of the (nonfluorescent) distamycin moiety of the hybrid, we have investigated the effect of addition of distamycin on the fluorescence emission spectra of the hybrid-DNA and the ellipticine-DNA complexes (Fig. 5). In both cases, a dramatic quenching of fluorescence is observed, leading to an almost complete extinction of the fluorescence of the ellipticine chromophore at high distamycin-DNA ratios. These fluorescence emission spectra were recorded with excitation at 318 nm. This wavelength corresponds to one of the isosbestic points observed upon titration of the ellipticine derivative (or the hybrid) with

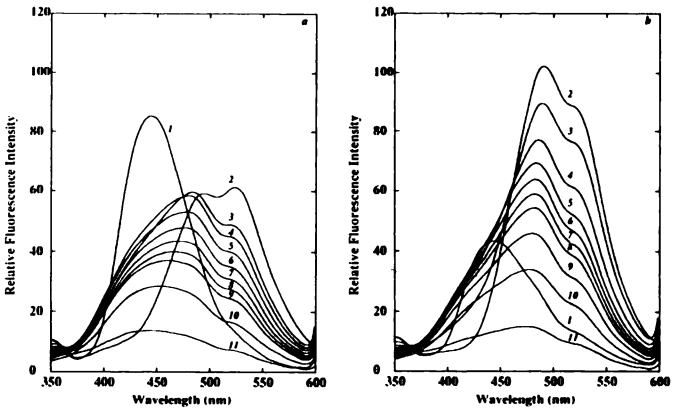

Fig. 5. Fluorescence emission spectra of the ellipticine derivative (a) and the hybrid (b), in the presence of increasing amounts of distamycin as competing ligand. To 3 ml of a drug-DNA complex solution (5 μM drug and 80 μM CT DNA, in 1 mM Tris·HCl buffer, pH 7.0), successive amounts of distamycin were added from a fresh 10 mM stock solution. Spectra were recorded after 10 min of equilibration, with an excitation wavelength of 318 nm. *Spectrum 1*, 5 μM free drug in solution; *spectrum 2*, drug-DNA complex (P/D = 16); *spectra 3–11*, drug-DNA complex in the presence of, respectively, 5, 10, 15, 20, 25, 30, 40, 50, and 100 μM distamycin.

DNA and is very close to the near-isosbestic point detected with distamycin (313 nm) (Fig. 2). Thus, the measured fluorescence variations do not result simply from changes in absorption of light energy.

At equal concentrations of distamycin and ellipticine (5 μM) (Fig. 5a, *spectrum 3*), the fluorescence spectrum of DNA-bound ellipticine is shifted by 10 nm toward the blue, indicating some displacement of bound ellipticine from its binding site. However, the spectrum is still red-shifted by 38 nm, compared with that of the free drug; thus, a large fraction of the drug is still bound to the DNA. Hence, the presence of equimolar distamycin does not abolish ellipticine binding.

Subsequent additions of distamycin result in larger blue shifts, together with substantial quenching of the fluorescence intensity. With a large excess of distamycin (100 μM), the spectrum of the ellipticine-DNA complex is very broad and presents a maximum close to that of free ellipticine, indicative of near-complete displacement of the intercalator.

The fluorescence intensity of the DNA-hybrid complex is also quenched by adding distamycin, although less dramatically than the fluorescence of the ellipticine-DNA complex (Fig. 5b). It appears that the ellipticine chromophore is not so easily displaced from its binding sites, and the quenching is not associated with a shift toward the fluorescence maximum of the free drug. Even at very high concentrations of distamycin (100 μM, versus 5 μM hybrid) (Fig. 5b, *spectrum 11*), the spectrum still corresponds to DNA-bound hybrid, whereas, under the same conditions, ellipticine alone is practically completely removed from its binding sites (Fig. 5a, *spectrum 11*).

Thermal denaturation. The ability of the hybrid to alter the thermal denaturation profile of DNA can be used as another indication of its propensity to bind to DNA. The effects of increasing concentrations of the hybrid and its component parts on the T_m of helix-to-coil transition of CT DNA and poly[d(AT)·d(AT)] are shown in Fig. 6. It was not possible to study the effects on poly[d(GC)·d(GC)], due to its high stability even at very low ionic strength. A large increase in the T_m of nucleic acids is observed for the hybrid, as well as for its parent compounds, using both CT DNA and poly[d(AT)·d(AT)].

The stabilization of the DNA double helix by binding of the hybrid increases smoothly with increasing D/P molar ratio up to a value of 0.3, after which the effect tends toward a plateau. With the two DNAs tested, the stabilizing action of the hybrid is substantial but always smaller than that of the parent compounds. Surprisingly, both distamycin and the ellipticine derivative exert similar stabilizing effects on CT DNA or poly[d(AT)·d(AT)], although ellipticine is endowed with substantial GC selectivity (see footprinting experiments). Thus, the results obtained with the two DNAs of different base composition cannot be interpreted in terms of preferential binding of the hybrid to AT- or GC-rich regions of DNA.

Distamycin- and hybrid-DNA complexes display, in each case, simple monophasic melting curves (the transition remains sharp even though the T_m changes). The ellipticine complex also shows monophasic curves at high D/P ratios (>0.2), but at low binding ratios biphasic curves are observed, and only the high melting temperature of the upper phase is reported in Fig. 6. It should be noted that the 1-aminoalkylamino ellipticine derivative gives a high ΔT_m, compared with values reported for the ellipticine base. The higher stabilization of the DNA helix is not surprising; it surely reflects interaction of the aminoalkylamino side chain with the DNA helix. The existence of cationic charge on the chromophore and/or its side chain is an important contributor to the total stabilization of any drug-DNA complex.

Unwinding. To confirm the mechanism of binding to DNA, the topoisomerization method was used to assay any changes induced in the DNA helix in the presence of the hybrid. The unwinding effects of the drugs can be frozen into the topology of closed circular DNA (typically plasmid DNA) in the presence of the enzyme topoisomerase I. After concomitant removal of the drug and enzyme, the degree and direction of change in topoisomer distributions are a direct reflection of drug-induced helical unwinding or overwinding. Any helical unwinding locked into a plasmid is replaced by compensatory negative supercoiling upon removal of the drug and enzyme. Helical overwinding is replaced by compensatory positive supercoiling. Using gel electrophoresis, adjacent topoisomer populations differing by single helical turns can be readily distinguished and changes can be quantitatively assayed by the band-counting method (30).

Fig. 7 shows the result of relaxing plasmid pKMΔ-98 in the

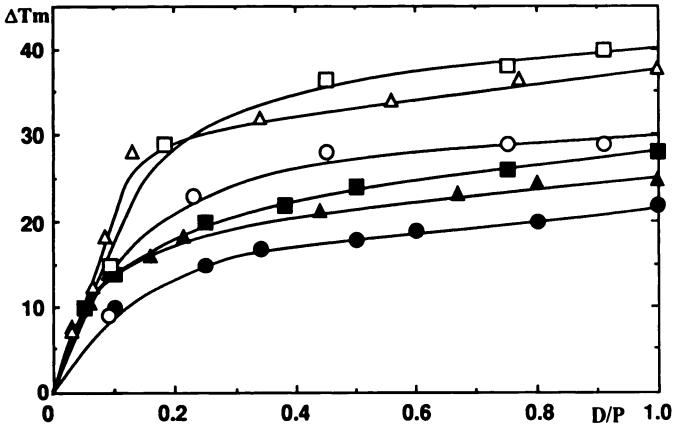

Fig. 6. Variation in melting temperature (ΔT_m in 0.1× standard saline citrate) of poly[d(AT)·d(AT)] (*open symbols*) and CT DNA (*closed symbols*) induced by the binding of distamycin (*squares*), the ellipticine derivative (*triangles*), and the hybrid (*circles*). In the absence of drug, the melting temperatures of CT DNA and poly[d(AT)·d(AT)] were 68° and 44°, respectively.

Fig. 7. Typical topoisomer patterns obtained after relaxation of the plasmid pKMΔ-98 (0.66 μg/20 μl; 3 units of enzyme), in the absence and presence of various concentrations of the hybrid, the ellipticine derivative, distamycin-A, and the reference compound, ethidium bromide. *Lane 1*, DNA control treated with topoisomerase I in the absence of drugs. The hybrid was used at 1, 2, 3, and 4 μM (*lanes 2–5*, respectively), the ellipticine derivative was used at 1.2, 2.4, 3.6, and 4.8 μM (*lanes 6–9*), distamycin-A was used at 4 and 20 μM (*lanes 10* and *11*), and ethidium bromide was used at 0.5, 1, and 2 μM (*lanes 12–14*).

presence of various concentrations of the hybrid, the ellipticine derivative, distamycin, and ethidium bromide for comparison. In the absence of drug, a topoisomer distribution centered close to +2 supercoils is seen (Fig. 7, *lane 1*), with the positive supercoils reflecting differences in ionic strength and temperature conditions between topoisomerization and electrophoresis (31). The presence of intercalator during the topoisomerization reaction initially results in a shift in topoisomer distributions towards zero supercoils. Such a shift is clearly seen for the hybrid (Fig. 7, *lane 2*) or ethidium bromide, a known intercalator (Fig. 7, *lane 12*). Higher drug concentrations during topoisomerization (Fig. 7, *lanes 3–5* for the hybrid, *lanes 6–9* for ellipticine, and *lanes 13* and *14* for ethidium bromide) result in increased amounts of negative supercoiling, with consequent enhanced electrophoretic mobility of the topoisomers. Under the conditions of electrophoresis used, positive and negative topoisomers are slightly out of phase and can be distinguished (compare Fig. 7, *lanes 10* and *11*). It can be seen that the supercoils induced by the hybrid are in phase with those produced by ethidium bromide (compare, for example, Fig. 7, *lanes 5* and *6*). Even at high concentrations, distamycin shows no such effect, with the mobility of plasmid DNA being similar in the absence (Fig. 7, *lane 1*) or presence (Fig. 7, *lanes 10* and *11*) of the antibiotic. Indeed, a weak tendency for the induction of positively supercoiled DNA (overwinding) was noticed, as previously reported for netropsin (32).

The center of each topoisomer distribution was estimated, and the change induced by addition of drug was calculated. The ratio of input ligand to plasmid DNA was used to calculate the unwinding induced per drug molecule added. This estimated unwinding, specific for these conditions of topoisomerisation, is presented in Table 1. The ellipticine derivative unwinds DNA to a similar extent as does the well characterized intercalating agent ethidium bromide. Such a high unwinding angle is a good criterion for DNA intercalation. The hybrid is approximately 50% less effective in promoting DNA unwinding than is ellipticine alone. This result might reflect the altered affinity of the hybrid, compared with the ellipticine derivative (Table 2), but is far more likely to reflect the influence of the distamycin moiety on the binding of the ellipticine chromophore. The ellipticine derivative shows ostensibly more efficient intercalation, reflected in a larger unwinding angle, than the hybrid. At first sight, the data suggest that intercalation of the ellipticine moiety in the hybrid molecule may not be as complete as it is with ellipticine alone.

ELD. In order to define the orientation of the ligand chromophore with respect to the DNA helix and to distinguish the binding processes of the two parts of the molecule, ELD experiments have been performed. In preliminary studies, the variation of reduced dichroism with the total D/P concentration ratio was determined, so as to characterize the binding process (data not shown). The modes of binding of the ligands were then analyzed on the basis of only the highest ELD values, obtained when the ligands are fully bound to DNA, i.e., at D/P ratios ranging from 0.05 to 0.2. At lower or higher D/P ratios, the measured ELD values fall significantly, due to the high concentration of DNA or to the appearance of unbound molecules in the solution, respectively.

The ELD spectrum of the hybrid-DNA complex is shown in Fig. 8 and is compared with those of the parent compounds. The hybrid compound gives negative dichroism values in the

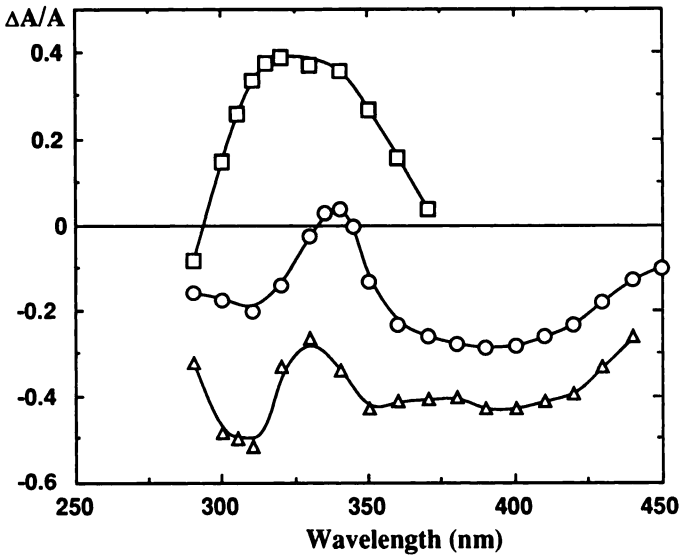

Fig. 8. Reduced ELD ($\Delta A/A$) spectra of distamycin-DNA (□), the ellipticine derivative-DNA (△), and the hybrid-DNA (○) complexes, at a D/P ratio of 0.1 and at 12.5 kV/cm.

310–320-nm region, although less negative than those measured with the ellipticine derivative alone. This is due to an important contribution of the distamycin moiety of the molecule in this wavelength region, so that the orientation of the ellipticine chromophore cannot be analyzed at this wavelength. The negative part of the ELD spectrum from 380 nm to 430 nm is due to the absorption of the ellipticine moiety, with a very minor contribution from the distamycin moiety (compare the UV spectra in Fig. 2). In this region, the hybrid exhibits negative ELD of amplitude slightly lower than that measured with ellipticine alone. This indicates that the ellipticine chromophore in the hybrid compound is not perfectly parallel to the plane of the DNA bases, in contrast to the case of ellipticine alone.

The binding configuration adopted by the distamycin part of the molecule cannot be fully estimated, due to a large overlap of its absorption spectrum with that of the ellipticine moiety. However, it is interesting to note that the positive ELD value measured at 340 nm with the hybrid-DNA complex (+0.028) corresponds approximately to the sum of the ELD values of the distamycin-DNA (+0.40) and ellipticine-DNA (−0.39) complexes at the same wavelength. Thus, binding of the distamycin part of the hybrid molecule may occur in a position similar to that adopted by the natural unsubstituted antibiotic.

For distamycin, the maximum ELD value found (+0.4) corresponds to an orientation angle <54.5° from the helix axis. The estimated angle is about 45° [determined according to a previously described procedure (13), based on a comparison of the reduced dichroism at a given field strength for the DNA bases and for the ligand at their respective absorption bands]. This result is in perfect agreement with the angle previously reported for distamycin (33).

The reduced dichroism of the DNA bases in the absence of drug was found to be −0.45 (at 260 nm and 12.5 kV/cm). The value for the ellipticine moiety bound to DNA ($\Delta A/A = -0.51$ at 310 nm) is nearly the same as for the DNA bases, indicating that this transition moment, located in the plane of the ellipticine chromophore, is closely parallel to the plane of the DNA base pairs. This is expected for intercalating agents.

Footprinting. A 160-base pair DNA fragment (the *tyr* T fragment) has been digested with DNase I in the presence or absence of the hybrid or its congeners, distamycin and ellipticine. All three drugs alter the digestion pattern, compared with that of the control reaction containing the DNA alone. The autoradiographs were analyzed by scanning with a microdensitometer, in order to quantify the intensity of each band, and then the data were transformed to produce a differential cleavage plot, as described in Materials and Methods. The pattern of protection of both strands of the *tyr* T DNA by the hybrid and the reference compounds is shown in Fig. 9.

It is obvious from this graph that distamycin and the ellipticine derivative exhibit different, virtually complementary, selectivity of binding. AT-rich regions of the DNA furnish major distamycin binding sites, such as positions 82–90 and 108–113 on both strands of the *tyr* TDNA. On the other hand, these distamycin-binding locations correspond to sites of enhanced cleavage of the ellipticine-bound DNA by DNase I. The

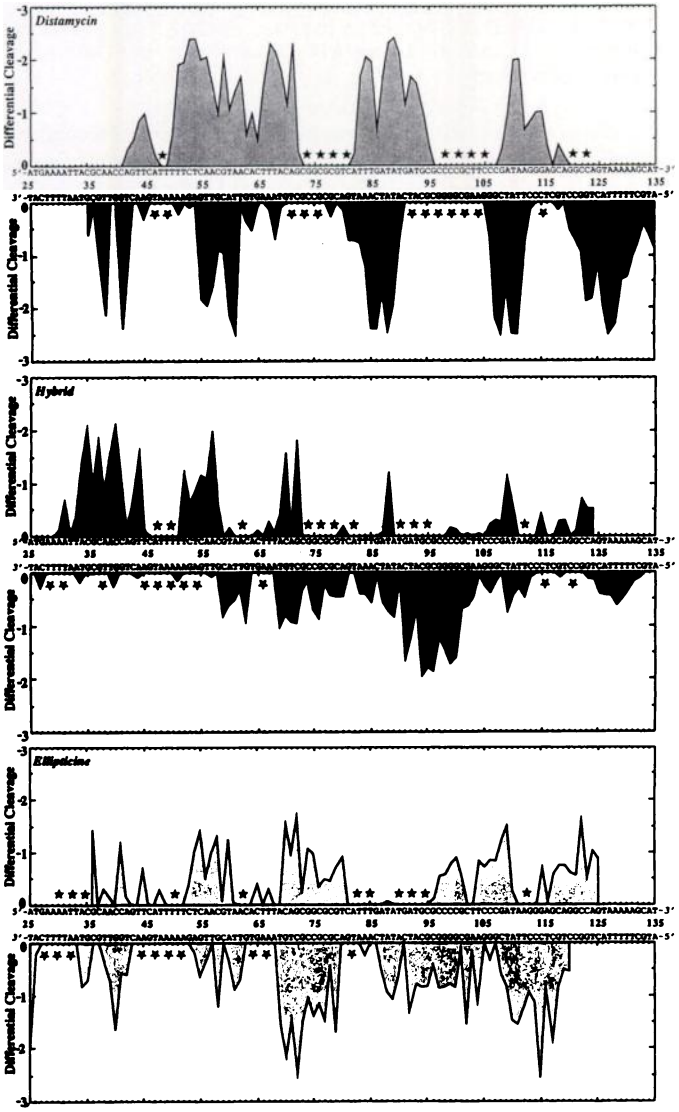

Fig. 9. Differential cleavage plots for distamycin-, hybrid-, and ellipticine derivative-induced differences in susceptibility of *tyr* T DNA to DNase I cleavage (10 μM of each drug). *Shaded areas*, sites where protection against DNAase I cleavage occurs, representing the possible binding sites of the drugs. ★, Sites of drug-induced enhanced cleavage by DNase I.

ellipticine derivative protects the GC-rich regions from cutting by DNase I (such as at positions 70–79 and 96–102). We note also that footprints produced by distamycin are 3′-shifted by 1 or 2 base pairs (as expected for DNase I cutting) but that no such obvious shifts are distinguishable with the ellipticine derivative.

Several regions protected by the hybrid are evident; enhanced cleavage is also evident at several other locations. The protection pattern found for the hybrid differs from that produced by distamycin, as well as that of the ellipticine derivative. Protection by the 3 hybrid occurs strikingly at the sequences 5′-CGCAACC-3′ (positions 35–41) and 5′-CTCAAC-3′ (positions 53–58) on the upper strand and the sequence 3′-CTACGCGGGGCGA-5′ (positions 91–103) on the bottom strand, which is very GC-rich and could well represent two overlapping binding sites. Various other minor sites are evident along the DNA sequence. It is interesting to observe that these sites are often detected on only one strand of the DNA, as if the complementary sequences located on the opposite strand were not favored as possible binding sites. This might suggest that DNA conformation, rather than sequence *per se*, is an important determinant of binding. Such a poor cross-strand correlation is unexpected, because DNase I binds across the minor groove of the helix, so that altering the binding (and cutting) on one strand would normally be expected to produce an equal effect on the opposite strand.

It should also be noted that, upon binding of the hybrid, numerous regions are rendered more susceptible to attack by DNase I than in the control. In fact, the protection pattern shown by the hybrid corresponds more closely, in some areas, to the sum of the regions of enhanced cleavage produced by both distamycin and ellipticine, rather than to the sum of their respective sites of binding. An explanation for this apparently peculiar behavior of the hybrid could reside in the need to use a high concentration of DNase I to observe cleavage of the DNA in its presence. Recently, we reported that the ellipticine derivative inhibited strongly the activity of the enzyme (20), presumably by stabilization of the enzyme-DNA complex, as reported for the topoisomerase II-DNA cleavable complex (34). The DNase I inhibition by the hybrid is even more pronounced at quite low drug concentration. Distamycin, however, did not inhibit DNase I. The potency of this hybrid drug to inhibit DNase I explains the difficulty in obtaining intense footprints.

Such selectivity of the hybrid as we can observe more closely resembles the pattern reported for the intercalating part of the drug, occurring essentially in GC-rich regions. Weak protection around position 128 (on the lower strand), corresponding to a strong distamycin binding site, is also revealed. It is clear, however, that nowhere along the length of the *tyr* T sequence accessible for analysis does the hybrid recognize a uniquely well defined sequence with high specificity.

In order to extend these observations, similar DNase I footprinting experiments were performed using a DNA fragment derived from the plasmid pBS (the *Ava*I-*Pvu*II restriction fragment), which contains different clusters of G and C residues (data not shown). Blockages were mainly confined to the sequences TCACTC and ACACAC. More pronounced were regions of enhanced cleavage in a run of A and T nucleotides. Similarly enhanced cleavage can be seen around position 50 on both strands of the *tyr* T DNA fragment, showing that binding

of this hybrid to homopolymeric sequences of A or T is clearly disfavored.

Discussion

Numerous synthetic DNA-intercalators and DNA-minor groove binders have proved promising as clinical anticancer and antiviral agents. Ellipticine derivatives (21) and distamycin analogues (8, 9) are good examples in each category. These compounds have been the subject of intensive study. Of particular interest is their molecular pharmacology and, especially, their modes of interaction with DNA or related cellular targets such as topoisomerases.

The properties of distamycin typify the characteristics of a minor groove binding agent, i.e., a weak hypochromic effect, strong stabilization of the DNA against thermal denaturation, positive linear dichroism of the DNA-bound drug, and no unwinding of supercoiled DNA (perhaps even a tendency to overwind it). On the other hand, various criteria for intercalative binding have been verified for the ellipticine derivative, i.e., high bathochromic and hypochromic effects, stabilization of DNA to heat denaturation, negative linear dichroism of the DNA-bound drug (amplitude similar to that of the DNA bases), and unwinding of supercoiled DNA (close to that measured for ethidium).

The mechanism of binding of the hybrid cannot be defined so easily. Indeed, the putative involvement of two distinct binding processes results in manifestly greater complexity of the spectral properties of the hybrid. However, it is possible to obtain substantial information on the nature of the drug-DNA complex by using multiple complementary techniques and by studying the parent compounds under the same conditions.

The main information obtained from the electronic absorption and fluorescence spectra is that the binding behavior of the hybrid is close to that of its component ellipticine derivative. But these results, together with those showing marked stabilization of the DNA towards heat denaturation, do not evidence mere intercalation by the hybrid, uncomplicated by other modes of interaction. The competition experiments, monitored by fluorescence, are, likewise, informative and allow us to evaluate the influence of distamycin (as competitor) on the binding of the hybrid and the ellipticine derivative.

Distamycin can cover about five DNA base pairs. Using 5 μM concentrations of both distamycin and ellipticine and 80 μM DNA (Fig. 5a, *spectrum 3*), only a small fraction of the base pairs could be in direct contact with distamycin, leaving the majority of the DNA free. Thus, if the only effect of distamycin were direct competition for ellipticine binding sites, the spectral properties of the ellipticine-DNA complex should not be greatly modified, unlike what we observed. Moreover, direct competition between distamycin and the ellipticine derivative for identical binding sites is very unlikely, in view of the footprinting data. The observed displacement of the ellipticine derivative may be ascribed to significant distamycin-induced conformational changes surrounding its binding sites and/or to some other effect(s) preventing the structural changes needed to accommodate intercalation by the ellipticine chromophore. This result is in perfect agreement with previous competition experiments, where it was shown that distamycin drastically reduces the affinity of ethidium bromide for DNA (35).

The hybrid shows rather different behavior upon competition with increasing amounts of distamycin. The ellipticine moiety of the drug remains more tenaciously bound to DNA and is only partially removed by a large excess of competitor. It is noteworthy that the hybrid, whose affinity for DNA is comparable to that of the ellipticine derivative (Table 2), requires higher concentrations of competitor to be displaced from its binding sites than does the intercalator alone. Because the two drugs differ only by the presence of the distamycin moiety, we may conclude that this difference in susceptibility to displacement is indeed due to the binding of the distamycin part of the hybrid to DNA. The insertion of the ellipticine chromophore must be somehow stabilized by the neighboring distamycin moiety. ELD experiments buttress this contention, although our attempts to measure the binding parameters directly do not reveal any very large effect.

The role of distamycin-induced DNA conformational changes is harder to evaluate in the case of competition between distamycin and the hybrid-DNA complex, because the DNA is subject to intense constraints upon binding of the hybrid and, in particular, of its distamycin moiety. If we assume that, in this case, the spectral changes do not result from indirect competition (through DNA structure perturbations), can they result from direct competition for identical binding sites? This latter possibility is not excluded by the footprinting results, even if binding of the hybrid to AT-rich regions of the DNA is not evident.

A crystallographic study (36) has shown that ellipticine derivatives intercalate with the quaternizable nitrogen of the pyridine ring pointing toward the major groove. Assuming that the same requirement for orientation of the chromophore applies to the hybrid, the position of the linking chain at position 1 might favor major groove binding. However, experiments with bacteriophage T_4 DNA, in which the major groove is glycosylated at cytidine residues (37), gave results identical to those for CT DNA.[1] This supports minor groove binding but does not allow us to clarify fully the geometry of the binding reaction. It does, however, suggest that direct interference (by added distamycin) with the lodging of the distamycin tail of the hybrid in the minor groove is a realistic possibility.

The ability of the hybrid drug to intercalate is also supported by the topoisomerization data. The drug unwinds DNA. The lower unwinding angle calculated for the hybrid, compared with that determined for ellipticine, may suggest partial intercalation of the drug or "off-setting" of ellipticine-induced unwinding by a small amount of concomitant overwinding by the distamycin moiety (see Ref. 32). In any case, the unwinding induced by different intercalators, even closely related ones, is not necessarily the same (38).

The results from the ELD experiments leave little room for doubt that the hybrid binds to DNA by both intercalation and groove binding. However, the intensity of the negative dichroism clearly shows that the orientations of the ellipticine chromophore in the hybrid and the ellipticine derivative alone, when bound to DNA, differ by some 10°. This difference suggests that intercalation of the ellipticine chromophore of the hybrid might not be complete or, at any rate, that its insertion may be associated with a certain amount of strain.

In a previous study on the binding of a netropsin-acridine hybrid drug (13), we demonstrated the weak intercalation of the acridine ring, whereas the acridine chromophore alone

[1] Unpublished observations.

intercalated fully. In the present case, we have used a longer and more flexible spacer in order to allow complete kinking of the drug, presumed necessary for simultaneous intercalation and groove binding. The results of Eliadis *et al.* (11) suggested that a polymethylene linker of three units in length should provide an optimum fit for such dual binding. Yet, despite the increased degree of intercalation of the ellipticine hybrid, relative to the acridine hybrid drug, it appears that full intercalation may still not be obtained. The outstanding question is, thus, whether the DNA can really accommodate binding of two very different functional moieties at neighboring sites. Studies with acridines linked to an oligonucleotide have revealed that intercalation and major groove binding can take place at juxtaposed sites (39). In that work, the linker with five methylene groups between the oligonucleotide and the acridine ring was shown to give better interaction with the DNA than a linker having only three units. Increasing the length of the linker in our case could also be beneficial. There is reason to believe that similar constraints may operate within the minor groove, because netropsin (an AT-specific minor groove binder) and actinomycin D (a GC-specific intercalator) can bind in close proximity along the DNA chain (40). In any case, we can expect the DNA to support alterations in conformation within a short distance.

Our efforts to discern the best configuration that will allow formation of the drug-DNA complex have been based on the assumption that the DNA is in the B conformation. It is likely, however, that upon binding the hybrid forces the DNA to adopt a new conformation (at least locally). Indeed, hyperreactivity of the drug-bound DNA towards diethylpyrocarbonate (data not shown) suggests that DNA conformational changes do occur. Thus, the DNA may well be switched to a non-B conformation in which the bases are not oriented perpendicularly to the helix axis. Under such circumstances, it is possible that the measured orientation of the ellipticine chromophore of the hybrid reflects a true intercalation between slightly tilted base pairs.

It is interesting to note that the sites of intercalation of the hybrid molecule seem to dominate the footprinting pattern, compared with the sites of distamycin binding (AT-rich sites). In contrast, previous studies by us (12, 13) and others (11), with netropsin-acridine hybrids, showed that the minor groove binding sites were easily revealed but that the sites of intercalation tended to remain cryptic or unobserved by footprinting. A possible explanation, as yet purely conjectural, for this feature is that the drug may selectively recognize a sequence that happened not to be present in the DNA used in the present study. Experiments are currently underway, using various DNAs having different nucleotide arrangements, to determine whether such selective recognition features exist.

In summary, the results of a variety of tests establish that the hybrid binds to DNA by both intercalation and groove binding (presumably in the minor groove). The exact geometry of the hybrid-DNA complex is far from fully understood. Studies to determine further the exact nature of this structure are continuing and will be reported in due course.

The design of minor groove binding-intercalating agents similar to the one described here presents new possibilities for interfering with biological processes such as replication and transcription. This strategy could ultimately lead to clinically more effective antitumor and antiviral drugs. Moreover, by synthesis of additional hybrids of this type, there should emerge a picture from which general principles for the design of sequence-specific DNA-binding drugs can be discerned.

Acknowledgments

The authors thank Dean Gentle for his excellent technical assistance. We are especially grateful to Dr. J. M. Smith of the Medical Research Council Laboratory of Molecular Biology (Cambridge) for instruction in the use of the microdensitometer and to Sir Aaron Klug and Dr. Smith for providing access to computer facilities.

References

1. Bishop, J. M. The molecular genetics of cancer. *Science (Washington D. C.)* **235**:305–311 (1987).
2. Berg, O. G., and P. H. von Hippel. Selection of DNA binding sites by regulatory proteins. *Trends Biochem. Sci.*207–211 (1988).
3. Dervan, P. B. Design of sequence-specific DNA-binding molecules. *Science (Washington D. C.)* **232**:464–471 (1986).
4. Nielsen, P. E. Sequence-selective DNA recognition by synthetic ligands. *Bioconjugate Chem.* **2**:1–12 (1991).
5. Bowler, B. E., K. J. Ahmed, W. I. Sundquist, L. S. Hollis, E. E. Whang, and S. Lippard. Synthesis, characterization, and DNA-binding properties of (1,2-diaminoethane)platinum(II) complexes linked to the DNA intercalator acridine orange by trimethylene and hexamethylene chains. *J. Am. Chem. Soc.* **111**:1299–1306 (1989).
6. Koyama, M., K. Takahashi, T. C. Chou, Z. Darzynkiewicz, J. Kapucinski, T. R. Kelly, and K. A. Watanabe. Intercalating agents with covalent bond forming capability: a novel type of potential anticancer agents. 2. Derivatives of chrysophanol and emodin. *J. Med. Chem.* **32**:1594–1599 (1989).
7. Prakash, A. S., W. A. Denny, T. A. Gourdie, K. K. Valu, P. D. Woodgate, and L. P. G. Wakelin. DNA-directed alkylating ligands as potential antitumor agents: sequence-specificity of alkylation by intercalating aniline mustards. *Biochemistry* **29**:9799–9807 (1990).
8. Krowicki, K., J. Balzarini, E. De Clercq, R. A. Newman, and J. W. Lown. Novel DNA groove binding alkylators: design, synthesis, and biological evaluation. *J. Med. Chem.* **31**:341–345 (1988).
9. Arcamone, F. A., F. Animati, B. Barbieri, E. Configliacchi, R. D'Alesio, C. Geroni, F. C. Giuliani, E. Lazzari, M. Menozzi, N. Mongelli, S. Penco, and M. A. Verini. Synthesis, DNA-binding properties, and antitumor activity of novel distamycin derivatives. *J. Med. Chem.* **32**:774–778 (1989).
10. Church, K. M., R. L. Wurdeman, Y. Zhang, and B. Gold. *N*-(2-Chloroethyl)-*N*-nitrosoureas bound to nonionic and monocationic lexitropsin dipeptides: synthesis, DNA affinity binding characteristics, and reactions with ^{32}P-end-labeled DNA. *Biochemistry* **29**:6827–6838 (1990).
11. Eliadis, A., D. R. Phillips, J. A. Reiss, and A. Skorobogaty. The synthesis and DNA footprinting of acridine-linked netropsin and distamycin bifunctional mixed ligands. *J. Chem. Soc. Chem. Commun.* 1049–1052 (1988).
12. Bailly, C., N. Pommery, R. Houssin, and J.-P. Hénichart. Design, synthesis, DNA-binding and biological activity of a series of DNA minor groove binding intercalating drugs. *J. Pharm. Sci.* **78**:910–917 (1989).
13. Bailly, C., N. Helbecque, P. Colson, C. Houssier, K. E. Rao, R. G. Shea, J. W. Lown, and J.-P. Hénichart. Molecular recognition between oligopeptides and nucleic acids: DNA sequence specificity and binding properties of an acridine-linked netropsin hybrid ligand. *J. Mol. Recognition.* **3**:26–35 (1990).
14. Subra, F., S. Carteau, J. Paoletti, C. Paoletti, C. Auclair, D. Mrani, G. Gosselin, and J. L. Imbach. Bis(pyrrolecarboxamide) linked to intercalating chromophore oxazolopyridocarbazole (OPC): selective binding to DNA and polynucleotides. *Biochemistry* **30**:1642–1650 (1991).
15. Neidle, S., L. H. Pearl, and J. V. Skelly. DNA structure and perturbation by drug binding. *Biochem. J.* **243**:1–13 (1987).
16. Kopka, M. L., C. Yoon, D. Goodsell, P. Pjura, and R. E. Dickerson. The molecular origin of DNA-drug specificity in netropsin and distamycin. *Proc. Natl. Acad. Sci. USA* **82**:1376–1380 (1985).
17. Kohn, K. W., M. J. Waring, D. Glaubiger, and C. A. Friedman. Intercalative binding of ellipticine to DNA. *Cancer Res.* **35**:71–76 (1975).
18. Zwelling, L. A., S. Michaels, D. Kerrigan, Y. Pommier, and K. W. Kohn. Protein-associated deoxyribonucleic acid strand breaks in mouse leukemia L1210 cells by ellipticine and 2-methyl-9-hydroxyellipticinium. *Biochem. Pharmacol.* **31**:3261–3267 (1982).
19. Auclair, C., B. Dugué, B. Meunier, and C. Paoletti. Peroxidase-catalyzed covalent binding of the antitumor drug N^2-methyl-9-hydroxyellipticinium to DNA *in vitro*. *Biochemistry* **25**:1240–1245 (1986).
20. Bailly, C., C. OhUigin, C. Rivalle, E. Bisagni, J.-P. Hénichart, and M. J. Waring. Sequence selective binding of an ellipticine derivative to DNA. *Nucleic Acids Res.* **15**:491–507 (1990).
21. Larue, L., C. Rivalle, G. Muzard, C. Paoletti, E. Bisagni, and J. Paoletti. A new series of ellipticine derivatives (1-(alkylamino)-9-methoxyellipticine): synthesis, DNA binding, and biological properties. *J. Med. Chem.* **31**:1951–1956 (1988).
22. Fox, K. R., and M. J. Waring. Nucleotide sequence binding preferences of nogalamycin investigated by DNase I footprinting. *Biochemistry* **25**:4349–4356 (1986).
23. Chaires, J. B., K. R. Fox, J. E. Herrera, M. Britt, and M. J. Waring. Site and

sequence specificity of the daunomycin-DNA interaction. *Biochemistry* **26**:8227–8236 (1987).
24. McGhee, J. D., and P. H. von Hippel. Theoretical aspects of DNA-protein interaction: co-operative and non-co-operative binding of large ligands to a one-dimensional homogeneous lattice. *J. Mol. Biol.* **86**:469–489 (1974).
25. Leatherbarrow, R. J. Using linear and non-linear regression to fit biochemical data. *Trends Biochem. Sci.* **15**:455–458 (1990).
26. OhUigin, C., D. J. McConnell, J. M. Kelly, and W. J. M. Van der Putten. Methylene blue photosensitised strand cleavage of DNA: effects of dye binding and oxygen. *Nucleic Acids Res.* **15**:7411–7427 (1987).
27. Smith, J. M., and D. J. Thomas. Quantitative analysis of one-dimensional gel electrophoresis profiles. *CABIOS* **6**:93–99 (1990).
28. Dodin, G., M.-A. Schwaller, J. Aubard, and C. Paoletti. Binding of ellipticine base and ellipticinium cation to calf-thymus DNA: a thermodynamic and kinetic study. *Eur. J. Biochem.* **176**:371–376 (1989).
29. Zimmer, C., and U. Wahnert. Non-intercalating DNA-binding ligands: specificity of the interaction and their use as tools in biophysical, biochemical and biological investigations of the genetic material. *Prog. Biophys. Mol. Biol.* **47**:31–112 (1986).
30. Keller, W. Determination of the number of superhelical turns in simian virus 40 DNA by gel electrophoresis. *Proc. Natl. Acad. Sci. USA* **72**:4876–4880 (1975).
31. Anderson, P., and W. Bauer. Supercoiling in closed circular DNA: dependence upon ion type and concentration. *Biochemistry* **17**:594–601 (1978).
32. Snounou, G., and A. D. B. Malcolm. Production of positively supercoiled DNA by netropsin. *J. Mol. Biol.* **167**:211–216 (1983).
33. Dattagupta, N., M. Hogan, and D. M. Crothers. Interaction of netropsin and distamycin with deoxyribonucleic acid: electric dichroism study. *Biochemistry* **19**:5998–6005 (1980).
34. Tewey, K. M., G. L. Chen, E. M. Nelson, and F. Liu. Intercalative antitumor drugs interfere with the breakage-reunion reaction of mammalian DNA topoisomerase II. *J. Biol. Chem.* **259**:9182–9187 (1984).
35. Hogan, M., N. Dattagupta, and D. M. Crothers. Transmission of allosteric effects in DNA. *Nature (Lond.)* **178**:521–524 (1979).
36. Jain, S. C., K. K. Bhandary, and H. M. Sobell. Vizualization of drug-nucleic acid interactions at atomic resolution. *J. Mol. Biol.* **135**:813–840 (1979).
37. Erickson, R. L., and W. Szybalski. The Cs_2SO_4 equilibrium density gradient and its application for the study of T-phage DNA glycosylation and replication. *Virology* **22**:11–18 (1964).
38. Waring, M. J. Variation of the supercoils in closed circular DNA by binding of antibiotics and drugs: evidence for molecular models involving intercalation. *J. Mol. Biol.* **54**:247–279 (1970).
39. Asseline, U., M. Delarue, G. Lancelot, F. Toulmé, N. T. Thuong, T. Montenay-Garestier, and C. Hélène. Nucleic acid-binding molecules with high affinity and base sequence specificity: intercalating agents covalently linked to oligonucleotides. *Proc. Natl. Acad. Sci. USA* **81**:3297–3301 (1984).
40. Wartell, R. M., J. E. Larson, and R. D. Wells. The compatibility of netropsin and actinomycin binding to natural deoxyribonucleic acid. *J. Biol. Chem.* **250**:2698–2702 (1975).

Send reprint requests to: Dr. Michael Waring, Department of Pharmacology, University of Cambridge, CB2 1QJ Cambridge, UK.